Synthesis, structural characterization, and antimicrobial efficiency of sulfadiazine azo-azomethine dyes and their bi-homonuclear uranyl complexes for chemotherapeutic use

Abdalla M. KHEDR[1,2,*], **Fawaz A. SAAD**[1]
[1]Chemistry Department, College of Applied Sciences, Umm Al-Qura University, Mecca, Saudi Arabia
[2]Chemistry Department, Faculty of Science, Tanta University, Tanta, Egypt

Abstract: Two sulfadiazine azo-azomethine dyes containing two active coordination centers and their bi-homonuclear UO_2(II)-complexes were synthesized for potential chemotherapeutic use. The ligands were prepared, starting from the coupling of sulfadiazine dizonium salt with acetylacetone, followed by condensation with ethylenediamine and 1,6-hexanediamine (HL^I and HL^{II}) using a modified literature procedure. The structures of the ligands and their UO_2(II)-complexes were elucidated by conventional and thermal gravimetric analyses, molar conductivity, magnetic susceptibility, and IR, UV-Vis, ^{1}H NMR, and mass spectra. The analytical and spectral data supported the binuclear formulation of the complexes with a 2:1 metal to ligand ratio and octahedral geometry. The molar conductance values of the UO_2(II)-complexes revealed their nonionic character. The ligands and their complexes were screened for their antibacterial activities towards the gram-positive *Staphylococcus aureus* and the gram-negative *Escherichia coli*, as well as their antifungal activities against *Aspergillus niger* and *Candida albicans*, in order to assess their antimicrobial potential. The results showed that metallization increases antimicrobial activity compared with the free ligands.

Key words: Sulfadiazine, azo-azomethine dyes, bi-homonuclear UO_2(II)-complexes, antimicrobial activities

1. Introduction

Sulfadiazine is a sulfonamide antibiotic and it is well known as one of the World Health Organization's List of Essential Medicines. It eliminates bacteria that cause infections by stopping the production of folate inside the bacterial cell, and is commonly used to treat urinary tract infections (UTIs).[1] Colorants, which include chromophores of dyes usually consisting of N=N, C=N, C=C aromatic and heterocyclic rings, containing oxygen, nitrogen, or sulfur, have been widely used as dyes owing to their versatility in various fields including high technology, such as biological staining, liquid crystalline displays, inkjet printers, textiles, and plastics, and in specialized applications, such as food, drug, cosmetic, and photochemical production.[2−5] Azo dyes are widely used in the textile industry and are the largest and most versatile group of synthetic organic dyes, with a tremendous number of industrial applications.[6] Schiff bases have also been shown to exhibit a broad range of biological activities, including antifungal, antibacterial, antimalarial, antiproliferative, anti-inflammatory, antiviral, and antipyretic properties.[7,8] Schiff base metal complexes have the ability to reversibly bind oxygen in epoxidation reactions,[9] biologically active compounds,[10] and catalytic hydrogenation of olefins.[11] Uranium

---

*Correspondence: abkhedr2010@yahoo.com

is a symbolic element as it is the last natural element and it is the most common element of actinides and has unique properties. Polynuclear metal complexes find wide applications in catalysis and materials science as well as biological applications.[12−16] Such complexes usually display unique spectroscopic and magnetic properties.[17−22] Keeping in mind the above facts, and in continuance of our interest in designing new ligands and complexes,[19−28] the synthesis, characterization, and antimicrobial efficiency of two sulfadiazine azo-azomethine dyes and their bi-homonuclear UO_2(II)-complexes are reported. The compounds are expected to combine the antibacterial activity of sulfadiazine azo-azomethine derivatives and antimicrobial activity of the metal ions, which constitute an important field of research due to their pronounced antimicrobial and fungicidal activities.[29]

2. Results and discussion

The structures of the ligands (HL^I and HL^{II}) and corresponding UO_2(II)-complexes were elucidated based on IR, UV-Vis, ^{1}H NMR, and mass spectra; molar conductivity; magnetic susceptibility; and conventional and thermal gravimetric analyses (Table 1).

Table 1. Physical and analytical data of sulfadiazine azo-azomethines (HL^I and HL^{II}) and their UO_2(II)-complexes[a] (**I** and **II**).

Molecular formula (Empirical formula)	Mol. Wt. (Cal. Mol. Wt.)	Color (Δ_m)	Analytical data			
			Found% (Calcd.)			
			%Hydrated H_2O	%Coordinated H_2O	%AcO⁻	%M
HL^I	403.00	Yellow (—)	—	—	—	—
($C_{17}H_{21}N_7O_3S$)	(403.46)	(—)				
$[(UO_2)_2L^I(AcO)_3(H_2O)]\cdot H_2O$	1155.00	Buff	1.52	1.51	15.29	40.96
($C_{23}H_{33}N_7O_{15}SU_2$) (**I**)	(1155.60)	(5.85)	(1.56)	(1.56)	(15.33)	(41.20)
HL^{II}	459.00	Yellow	—	—	—	—
($C_{21}H_{29}N_7O_3S$)	(459.57)	(—)				
$[(UO_2)_2L^{II}(AcO)_3(H_2O)]\cdot H_2O$	1211.00	F.buff	1.44	1.43	14.53	39.11
($C_{27}H_{41}N_7O_{15}SU_2$) (**II**)	(1211.78)	(6.55)	(1.49)	(1.49)	(14.62)	(39.29)

[a]The synthesized complexes decompose without melting above 278 °C.
The yield of the synthesized compounds was 80%–84%.
Mol. Wt. is the molecular weight obtained from mass spectra.
Δ_m is the molar conductance measured in Ohm^{-1} cm^2 mol^{-1}.

2.1. Solubility and molar conductance

The metal chelates $[(UO_2)_2L^I(AcO)_3(H_2O)]\cdot H_2O$ (**I**) and $[(UO_2)_2L^{II}(AcO)_3(H_2O)]\cdot H_2O$ (**II**) are stable in air and soluble in DMF and DMSO but insoluble in water and common organic solvents. Single crystals of the metal chelates could not be isolated from any organic solution. The molar conductance values of the complexes equal 5.85 and 6.55 Ω^{-1} cm^2 mol^{-1} for **I** and **II**, respectively, indicating that they are nonelectrolytes. This confirms that the anions are inside the coordination sphere of the metal ion.[30]

2.2. Conventional and thermal analyses

The thermal analysis results of the complexes **I** and **II** are in good agreement with the theoretical calculations. The uranium contents in the complexes were identified gravimetrically using the standard method.[31] A weighed

quantity of complex (0.4~0.5 g) was treated with a few drops of conc. H_2SO_4 and 1 mL of conc. HNO_3. It was heated until the organic matter decomposed and sulfur trioxide fumes came out. The same process was repeated three to four times to decompose the complex completely. Then it was dissolved in water and the resulting solution was used for analysis of the metal ion percentage. Uranium was precipitated as ammonium diuranate, followed by sufficient ignition to its respective oxide. The nature and contents of water molecules and acetate groups attached to the central metal ion were determined by conventional thermal decomposition studies.

In a conventional thermal analysis, UO_2(II)-complexes **I** and **II** were heated at four temperatures (100 °C, 200 °C, 300 °C, and 1000 °C) in a muffle furnace for ≈50 min. The resulting weights were determined. The weight loss at 100 °C can be attributed to loss of lattice water from the complexes. The weight loss at 200 °C is due to loss of coordinated water. The weight loss at 300 °C can be attributed to the removal of acetate groups. The weight of the final product after heating at 1000 °C corresponds to the formation of the metal oxide as a final product.[32]

Confirmation of the proposed molecular structure of the investigated complexes was carried out using TGA from which information on their properties, nature of intermediate, and final products of their thermal decomposition were obtained.[33] TGA curves were obtained for UO_2(II)-complexes **I** and **II**. The mass losses were calculated for the different decomposition steps and compared with those theoretically calculated for the suggested formula based on analytical and spectral results as well as molar conductance measurements. The results of TGA indicate the formation of metal oxide as the end product from which the metal content is calculated and compared with that obtained from analytical determination. The results obtained for the thermal decomposition patterns are presented in Table 2. The thermal decomposition of the complexes occurs through four steps. The water of hydration was removed within the 50–99 °C temperature range, while the coordinated water molecules were removed within the 130–178 °C range. The number of water molecules was determined from the percentage weight losses at these steps. The removal of coordinated acetate groups was observed within the 210–286 °C range. The complete decomposition of the organic ligands occurred at temperatures higher than 306 °C. The final product was the metal oxide.[34]

Table 2. Data obtained from TGA curves of UO_2(II)-complexes **I** and **II**.

Compound	% Loss in weight found (calcd.)	Temperature range (°C)	Assignment (thermal process)
$[(UO_2)_2L^I(AcO)_3(H_2O)]\cdot H_2O$ (**I**)	1.65 (1.56)	55–95	Loss of hydrated H_2O
$[(UO_2)_2L^I(AcO)_3(H_2O)]$	1.49 (1.56)	130–168	Removal of coordinated H_2O
$[(UO_2)_2L^I(AcO)_3]$	15.12 (15.33)	210–280	Elimination of coordinated acetate groups
$[(UO_2)_2L^I]$	31.84 (32.05)	310–1000	Complete decomposition of the complex and formation of metal oxide as a final product
$[(UO_2)_2L^{II}(AcO)_3(H_2O)]\cdot H_2O$ (**II**)	1.81 (1.49)	50–99	Loss of hydrated H_2O
$[(UO_2)_2L^{II}(AcO)_3(H_2O)]$	1.32 (1.49)	130–178	Removal of coordinated H_2O
$[(UO_2)_2L^{II}(AcO)_3]$	14.88 (14.62)	220–286	Elimination of coordinated acetate groups
$[(UO_2)_2L^{II}]$	34.97 (35.19)	306–1000	Complete decomposition of the complex and formation of metal oxide as a final product

2.3. TOF-mass spectral studies

Mass spectra are used in order to confirm the constitutions and purities of the prepared ligands and UO_2 (II)-complexes. The mass spectra of sulfadiazine azo-azomethine dyes showed accurate molecular ion peaks at m/z 403 and 459 for HL^I and HL^{II}, respectively, matched with the theoretical values. Moreover, the spectra of $[(UO_2)_2 L^I (AcO)_3 (H_2O)] \cdot H_2O$ and $[(UO_2)_2 L^{II} (AcO)_3 (H_2O)] \cdot H_2O$ displayed accurate molecular ion peaks at m/z 1155 and 1211, respectively, corresponding to the parent ion $[ML]^+$. Successive degradation of the target compound and appearance of different peaks due to various fragments are good evidence for the molecular structure of the investigated complexes.[19] The mass spectrum of complex **I** showed peaks at m/z 1155, 1137, 1119, 1060, 1001, and 942 corresponding to $[(UO_2)_2 L^I (AcO)_3 (H_2O)] \cdot H_2O$ (the molecular weight of complex cation), $[(UO_2)_2 L^I (AcO)_3 (H_2O)]$ (loss of the hydrated water molecule), $[(UO_2)_2 L^I (AcO)_3]$ (loss of two water molecules), $[(UO_2)_2 L^I (AcO)_2]$ (loss of two water molecules and one acetate group), $[(UO_2)_2 L^I (AcO)]$ (loss of two water molecules and two acetate groups), and $[(UO_2)_2 L^I]$ (loss of two water molecules and three acetate groups). New good evidence confirms the proposed structure of the complexes comes from the decomposition of complexes **I** and **II** via abstraction of the ligand, which give rise to the presence of a molecular ion peak attributable to $[L]^+$ (Scheme 1). This is common behavior for metal ion complexes containing different ligands (ML) that decompose through cleavage of the metal–ligand bond during the spray ionization process.[35]
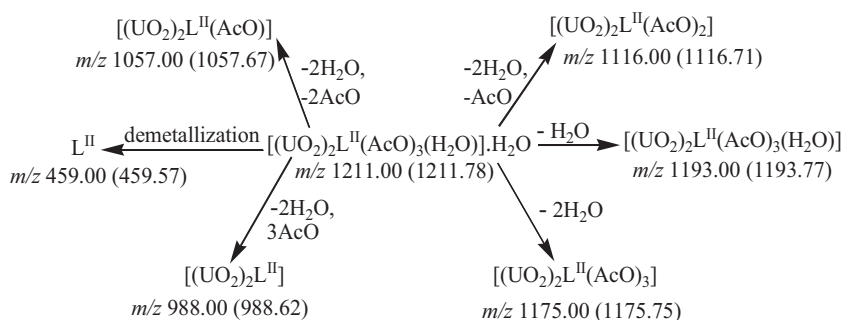
Scheme 1. Fragmentation pathways of $[(UO_2)_2 L^{II} (AcO)_3 (H_2O)] \cdot H_2O$ (**II**).

2.4. FT-IR spectral studies

A comparative study between the FT-IR spectra of the free ligands (HL^I and HL^{II}) and those of their UO_2 (II)-complexes **I** and **II** was conducted in order to investigate the mode of binding in the formed complexes (Table 3). The metal ions usually form bonds with Schiff base derivatives of sulfa-drugs through the Schiff base center or the sulfonamide part for mononuclear complexes, while for binuclear ones both centers contribute.[36] IR spectra of HL^I and HL^{II} displayed strong bands at 3423 and 3426 cm^{-1}, which can be attributed to the stretching vibration of OH, confirming enolization of C=O through keto-enol tautomerism (Scheme 2).[19] IR spectra of complexes **I** and **II** showed broad bands at 3426 cm^{-1}, which can be assigned to ν(OH) of water associated with complexes. The presence of water renders it difficult to confirm the deprotonation of the OH groups on complex formation from the stretching vibration.[37] Stretching vibration bands of aliphatic ν(C=N) appeared at 1581 cm^{-1}, whereas aromatic ν(C=N) bands appeared at 1630 and 1612 cm^{-1} in the spectra of HL^1 and HL^2, respectively. These bands have invariable shifts in the spectra of complexes **I** and **II**, indicating the coordination of the aromatic and aliphatic azomethine nitrogens to the metal ion in chelate formation.[38]

Sharp bands appeared around 1325 and 1155 cm^{-1} in the spectra of HL^{I} and HL^{II}, due to $\nu_{as}(SO_2N)$ and $\nu_s(SO_2N)$, respectively. These bands shifted slightly to higher or lower frequencies upon coordination to UO$_2$(II).[38] $\nu_{as}(OCO)$ and $\nu_s(OCO)$ of the acetate group in the uranyl complexes **I** and **II** are observed around 1495 and 1442 cm^{-1}, respectively. This revealed monodentate coordination of this group [$\Delta(OCO)$ = $\nu_{as}(OCO)$ – $\nu_s(OCO)$ < 100 cm^{-1})].[39] The medium intensity bands that appeared around 3356, 3259, 3041, 2938, 1651, 1409, 1261, and 683 cm^{-1} can be assigned to $\nu(NH_2)$, $\nu(NH)$, $\nu(CH\text{-aromatic})$, $\nu(CH_2)$, $\nu(C=O)$, $\nu(N=N)$, $\nu(S=O)$, and $\nu(C\text{-}S)$, respectively. These observations are supported by the appearance of two new nonligand bands at 640 cm^{-1} and around 502 cm^{-1} due to $\nu(M–O)$ and $\nu(M–N)$,[40] respectively. The characteristic $\nu_{as}(UO_2)$ band appeared near 843 cm^{-1} in the spectra of UO$_2$(II)-complexes **I** and **II**.[41] The previous studies,[19,20,36,37] and the IR spectral studies revealed that the ligands coordinate to the metal via a nitrogen atom of the pyrimidine ring, the oxygen atom of sulfonamide group, azomethine-N, and enolic OH formed through a keto–enol tautomerism of the C=O group (Scheme 2).

Table 3. IR spectral data (cm^{-1}) of HL^{I}, HL^{II}, and their UO$_2$(II)-complexes **I** and **II**.

No	$\nu(OH)$ [$\nu(NH)$]	$\nu(NH_2)$ [$\nu(CH_{arom})$]	$\nu(C=N_{arom})$ [$\nu(C=N_{azom})$]	$\nu(N=N)$ [$\nu(S=O)$]	$\nu_{as}(OCO)$ [$\nu_s(OCO)$]	$\nu(SO_2N)$	$\nu_{as}(UO_2)$ [$\nu_s(C\text{-}S)$]	$\nu(M\text{-}O)$ [$\nu(M\text{-}N)$]
HL^{I}	3423 [3355]	3257 [3038]	1630 [1581]	1409 [1261]	— [—]	1325, 1156	— [683]	— [—]
I	3426 [3358]	3258 [3042]	1623 [1594]	1410 [1263]	1495 [1442]	1326, 1155	843 [682]	640 [503]
HL^{II}	3426 [3357]	3259 [3039]	1612 [1582]	1409 [1262]	— [—]	1325, 1155	— [684]	— [—]
II	3426 [3358]	3262 [3041]	1623 [1594]	1409 [1263]	1494 [1442]	1326, 1155	843 [683]	640 [502]
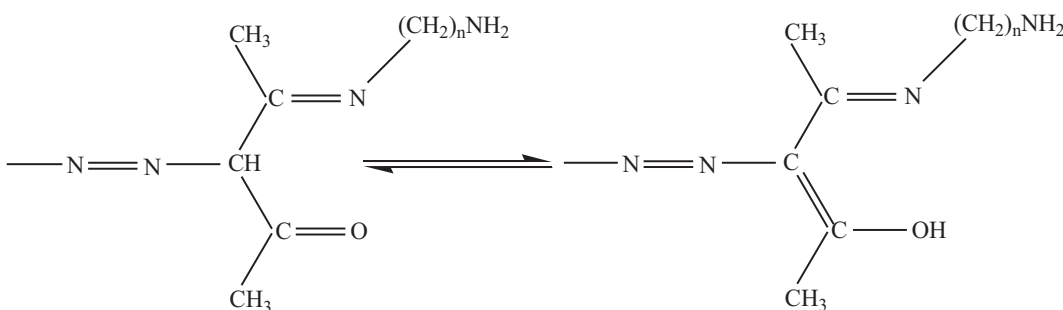
Scheme 2. Keto-enol tautomerism in sulfadiazine azo-azomethine dyes (HL^{I} and HL^{II}).

2.5. Electronic absorption spectra and magnetic susceptibility data

UV-Vis spectral results of sulfadiazine azo-azomethine dyes and their UO$_2$(II)-complexes in DMF solution are presented in Table 4. The spectra of HL^{I} and HL^{II} showed three bands. The first band appeared within the 292–304 nm range and can be attributed to the low energy $\pi - \pi^*$ transition corresponding to $^1L_b \leftarrow\, ^1A$ state of the phenyl ring. The second band appeared within the 360–390 nm range due to the $n - \pi^*$ transition. The third band appeared at the 440–462 nm range due to charge transfer transitions within the whole molecule.[42] The spectra of UO$_2$(II)-complexes **I** and **II** displayed a weak band at 478 nm and a highly intense band

271

near 303 nm, which are attributed to $^1\Sigma_g^+ \rightarrow^3 \pi_u$ transitions and charge transfer overlapping with $\pi - \pi^*$ transition, respectively.[43] The band occurring near 355 nm can be assigned to uranyl moiety because apical oxygen$\rightarrow f^o$(U) transition is being merged with the ligand band due to n$\rightarrow \pi^*$ transition as evident from broadness and intensity.[44] As expected, magnetic susceptibility data prove that UO_2(II)-complexes **I** and **II** are diamagnetic.[45]

Table 4. UV-Vis and ^{1}H NMR spectral data of HL^I, HL^{II}, and their UO_2(II)-complexes **I** and **II**.

No	UV-Vis spectra	^{1}H NMR spectra					
	(λ_{max} , nm)	δ_{OH}	δ_{CH-N}	δ_{Ar-H}	δ_{NH}	δ_{NH2}	δ of CH_3 groups
HL^I	292, 390, 440	11.13	7.03	7.71–7.62	9.95	9.23	4.13
I	303, 356,478	—	—	8.02–7.92	10.45	9.70	4.61
HL^{II}	304, 360, 462	11.21	7.28	7.92–7.80	10.05	9.44	4.58
II	302, 355, 478	—	—	7.96–7.86	10.28	9.55	4.90

2.6. ^{1}H NMR spectral studies

^{1}H NMR spectra of HL^I and HL^{II} were studied and compared with those of their UO_2(II)-complexes (**I** and **II**), in order to determine the center of chelation and replaceable hydrogen upon complex formation (Table 4). The ^{1}H NMR spectra of HL^I and HL^{II} and their UO_2(II)-complexes (**I** and **II**) are shown in Figures 1–4. Signals at 11.13 and 11.21 ppm due to δ_{OH} in the spectra of HL^I and HL^{II}, respectively, support the presence of OH produced from keto–enol tautomerism as concluded from IR spectra (Scheme 2). Furthermore, the aliphatic –CH—N– proton appeared as a singlet at 7.03 and 7.28 ppm in the spectra of free ligands. These signals disappeared in the ^{1}H NMR spectra of the complexes, denoting that complex formation occurs via deprotonation of the OH group.[46] The signals that appeared at 9.95; 10.05, 9.23; 9.44, 8.47; 8.64, 7.71–7.62; 7.92–7.80, 4.13; 4.58 and 3.25; 4.05 ppm due to δ_{NH}, δ_{NH2}, $\delta_{pyrimidine-H}$, $\delta_{benzene-H}$, δ_{CH3}, and δ_{CH2} in the free ligand spectra have downfield shifts in the spectra of the complexes due to increased conjugation on coordination, supporting coordination of ligands to UO_2(II) ion. The downfield shift of these signals is due to deshielding by UO_2(II), giving further support for the presence of the metal ions.[47] The ^{1}H NMR spectra of UO_2(II)-complexes **I** and **II** showed two new nonligand signals at 2.23 and 2.02 and 3.12 and 3.00 ppm for water and CH_3 from acetate, respectively.[20]

2.7. In vitro antibacterial and antifungal assay

The antimicrobial activity of any compound is a complex combination of steric, electronic, and pharmacokinetic factors. The action of the compound may involve the formation of a hydrogen bond through —N=C of the chelate or the ligand with the active centers of the cell constituents, resulting in interference with the normal cell process. The microbotoxicity of the compounds may be ascribed to the metal ions being more susceptible toward the bacterial cells than ligands.[48] The in vitro antimicrobial activities of the prepared sulfadiazine azo-azomethine dyes (HL^I and HL^{II}) and their UO_2(II)-complexes (**I** and **II**) were screened against *E. coli*, *S. aureus*, *A. flavus*, and *C. albicans* using the modified Kirby–Bauer disc diffusion method.[49] Standard drugs amphotericin B and tetracycline were tested for their antibacterial and antifungal activities in the same conditions and concentrations. UO_2(II)-complexes showed significant antimicrobial activities against the tested organisms compared with the free ligands (Table 5). Complexes **I** and **II** displayed high activity
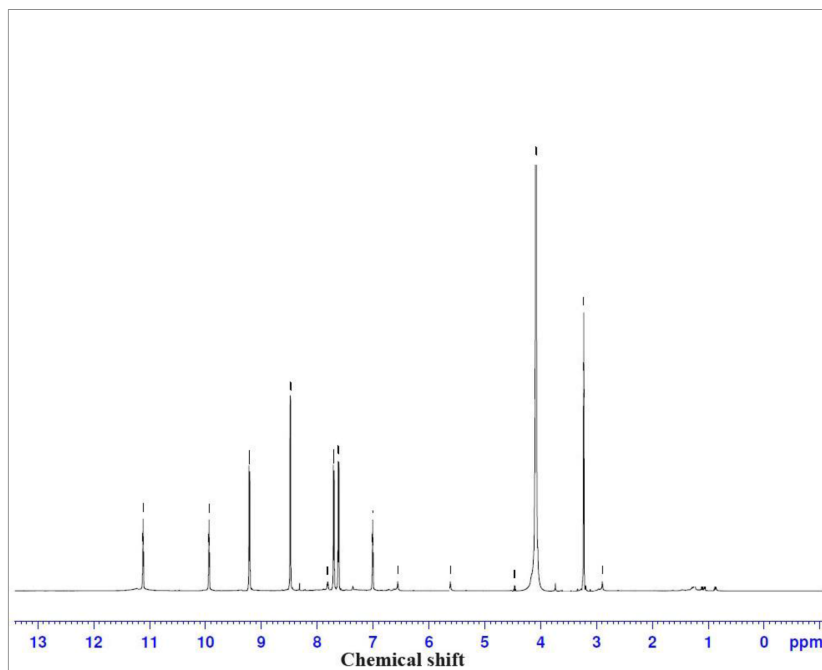
Figure 1. ^{1}H NMR spectrum of ligand HL^I.
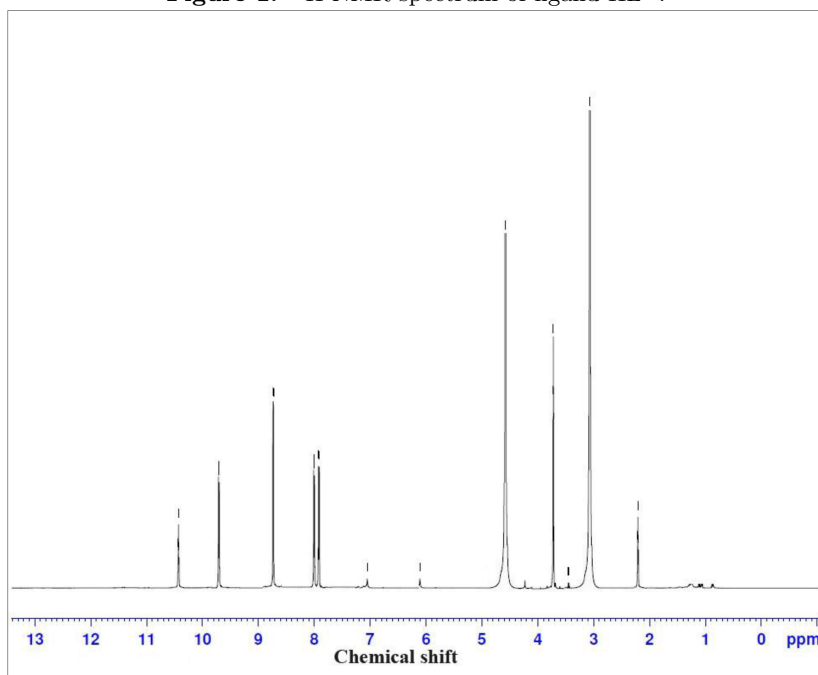
Figure 2. ^{1}H NMR spectrum of complex **I**.

against different types of tested bacteria. Moreover, complexes **I** and **II** exhibited moderate activity against *A. flavus*. Sulfadiazine azo-azomethine ligands (HL^I and HL^{II}) and complexes are inactive against *C. albicans*. Complexes **I** and **II** were less active compared with tetracycline and amphotericin B. The data prove the potential of complexes **I** and **II** as broad spectrum antibacterial agents. Furthermore, complexes **I** and **II** can be used as effective antifungal agents against multicellular fungi. The improved activities of the metal complexes
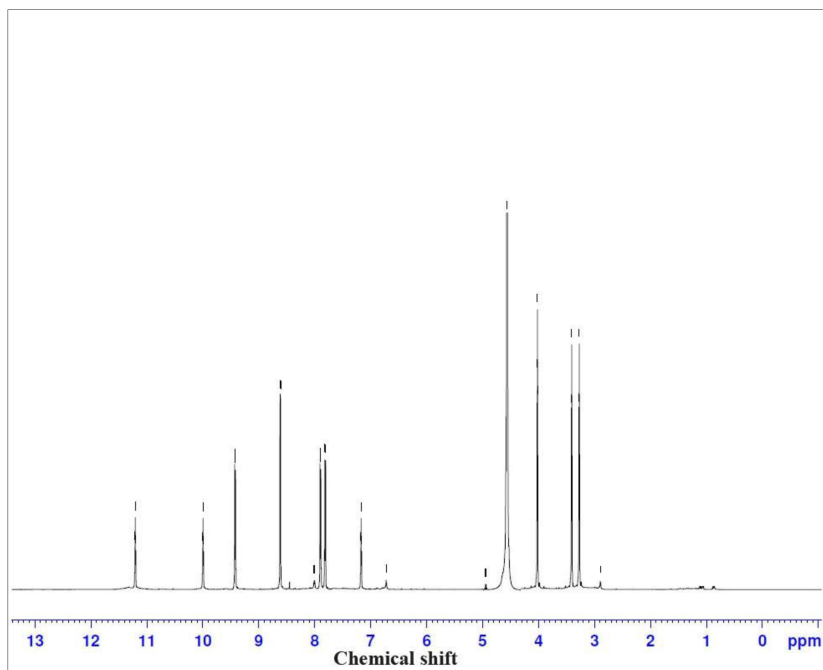
Figure 3. ^{1}H NMR spectrum of ligand HL^{II}.
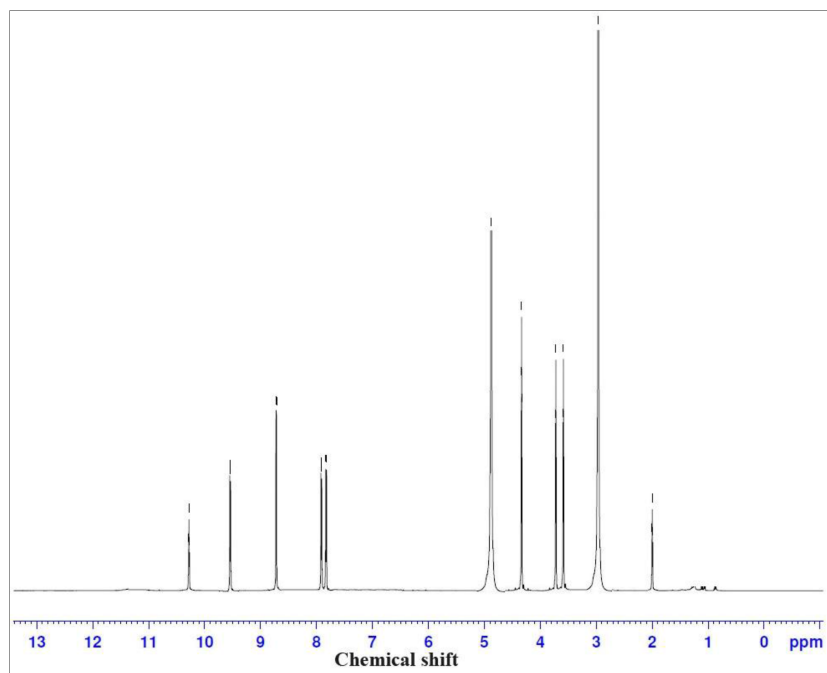
Figure 4. ^{1}H NMR spectrum of complex **II**.

compared with the free ligand can be explained on the basis of chelation theory.[50] This theory states that a decrease in the polarizability of the metal could enhance the lipophilicity of the complexes. This leads to a breakdown of the permeability of the cells, resulting in interference with normal cell processes.[51] This indicates that chelation tends to make the Schiff bases act as more powerful and potent antimicrobial agents, inhibiting the growth of bacteria and fungi more than the parent Schiff bases.[52] Therefore, it is claimed that the process of

chelation dominantly affects the biological activity of compounds that are potent against microbial and fungal strains. *S. aureus* was selected to represent gram-positive bacteria, whereas *E. coli* was selected as the backbone of gram-negative bacteria. *C. albicans* represented the unicellular fungi, while *A. flavus* was selected as a higher fungus representing multicellular fungi. Therefore, the selected organisms represent a broad spectrum of test organisms. The obtained results prove the usefulness of complexes **I** and **II** as broad spectrum antimicrobial agents.

Table 5. Antibacterial and antifungal activities of HL^I, HL^{II}, and their UO_2(II)-complexes **I** and **II**.

Compound	Inhibition zone diameter (mm mg^{-1} sample)			
	E. coli (G$^-$)	*S. aureus* (G$^+$)	*A. flavus* (fungus)	*C. albicans* (fungus)
Control: DMSO	0.0	0.0	0.0	0.0
Tetracycline (Antibacterial agent)	33.0	30.0	—	—
Amphotericin B (Antifungal agent)	—	—	20.0	20.0
HL^I	15.0	16.0	0.0	0.0
Complex **I**	18.0	20.0	10.0	0.0
HL^{II}	13.0	16.0	0.0	0.0
Complex **II**	20.0	21.0	11.0	0.0

3. Experimental

3.1. Materials and measurements

All chemicals used in the synthesis were of reagent grade and used without further purification. All solvents were of reagent grade and purified according to the standard procedure. The thermal gravimetric analysis (TGA) of UO_2(II)-complexes was performed using a Shimadzu TG-50 thermal analyzer from ambient temperature up to 800 °C under nitrogen as atmosphere with a heating rate of 10 °C/min. Molar conductance of the complexes was determined in DMSO (10^{-3} M) at room temperature using a Jenway (model 4070) conductivity meter. Matrix Assisted Laser Desorption/Ionization Time-of-Flight (MALDI-TOF) mass spectra were obtained by the aid of a BRUKER Auto flex II LRF20 spectrometer using dithranol as a matrix. Infrared spectra of the ligand and its metal complexes were recorded on a FT-IR Bruker Tensor 27 spectrophotometer, within 4000–400 cm^{-1} range as KBr discs (at Central Laboratory, Tanta University, Egypt). The electronic spectra were recorded on a Shimadzu 240 UV-Visible spectrophotometer. Magnetic susceptibility measurements of the metal complexes in powder form were carried out on a Guoy balance using mercuric tetrathiocyanato-cobaltate(II) as the magnetic susceptibility standard. ^{1}H NMR spectra were measured using a Bruker DMX 750 (500 MHz) spectrometer in DMSO-d$_6$ as the solvent and tetramethylsilane as the internal standard. Chemical shifts of ^{1}H NMR were expressed in parts per million (ppm, δ units), and the coupling constant was expressed in hertz (Hz).

3.2. Preparation of sulfadiazine azo-azomethine dyes

Sulfadiazine azo-azomethine dyes (HL^I and HL^{II}) were prepared according to the following procedures. 4-(3-Pentyl-2,4-dione)-N-pyrimidin-2-yl-benzenesulfonamide was synthesized according to a modified procedure.[53] To a solution of acetylacetone (1.00 g, 10 mmol) in 30 mL of ethanol was added sodium acetate (3.0 g). The mixture was cooled to 0 °C for 10 min and a cooled solution of sulfadiazine dizonium chloride (prepared from 10 mmol of sulfadiazine (2.50 g) and the appropriate quantities of HCl and NaNO$_2$) was added under stirring.

The stirring was continued for 1 h after which the solid was collected, washed with 2×10 mL of water and 2×10 mL of ethanol, and dried in air. The obtained sulfadiazine azo dye was recrystallized several times from ethanol.

HL^I and HL^{II} were prepared using a procedure taken from the literature[53] and modified. A mixture of 10 mmol of 4-(3-pentyl-2,4-dione)-N-pyrimidin-2-yl-benzenesulfonamide (3.61 g) and ethylenediamine (0.60 g) or 1,6-hexanediamine (1.16 g) was dissolved in absolute ethanol (50 mL) with a few drops of piperidine as a catalyst. The mixture was refluxed at 80 °C for 10–12 h. The resulting solid product was collected by filtration and washed several times with hot ethanol. The different synthetic procedures for preparation of HL^I and HL^{II} are presented in Scheme 3.
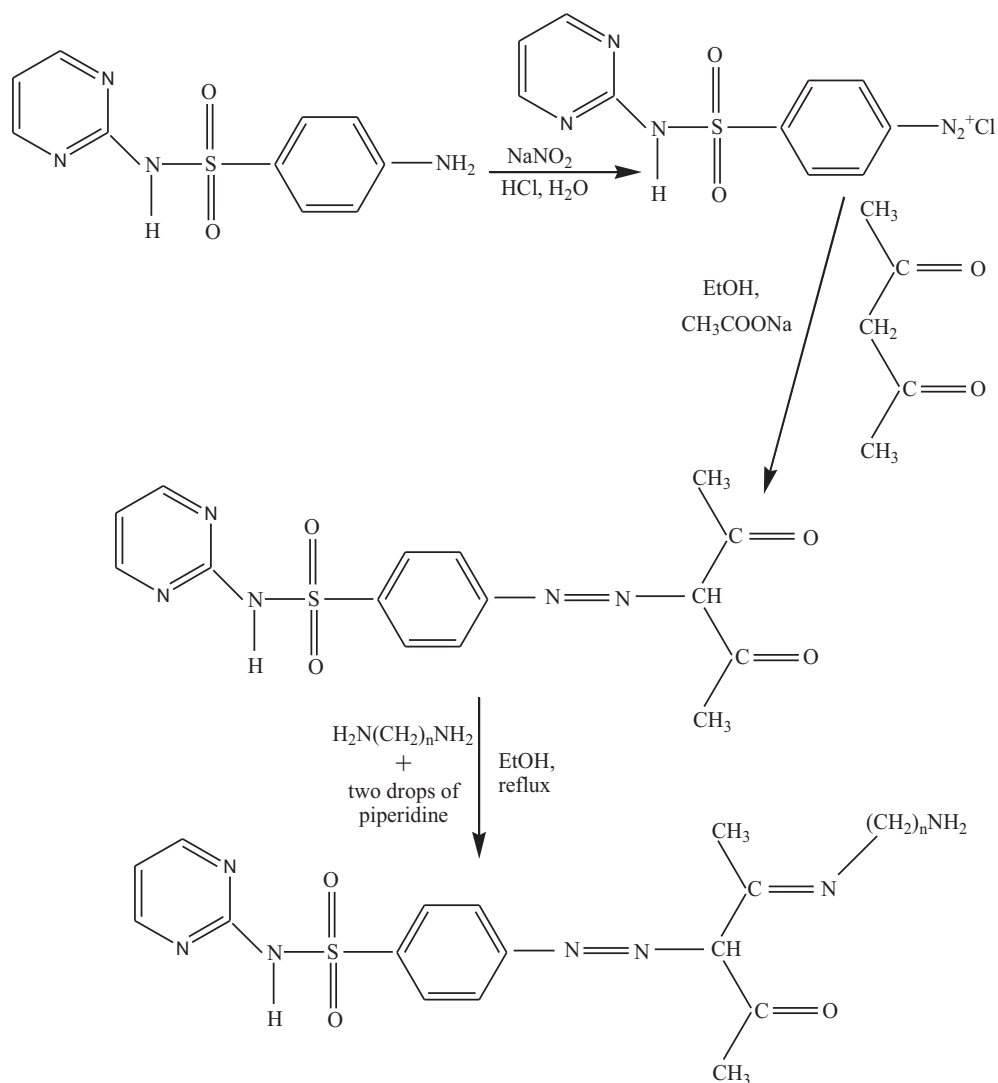
Scheme 3. Procedures for preparation of sulfadiazine azo-azomethines dyes [HL^I (n = 2) and HL^{II} (n = 6)].

3.3. Synthesis of the metal complexes

UO_2 (II)-complexes **I** and **II** were synthesized using the well-known reflux-precipitation method. Uranyl acetate dihydrate solution (2 mmol in 50 mL of water/ethanol mixture (50%, V/V)) was added dropwise to an ethanolic

solution of sulfadiazine azo dye HL^I or HL^{II} (1 mmol in 50 mL of ethanol). Then the resulting mixture was refluxed for 14–16 h on a water bath. The complexes precipitated during the reaction were filtered off and washed several times with hot ethanol, and then dried in a vacuum over anhydrous calcium chloride. The reaction yield was found to be 80%–84%. The purities of the complexes were checked by TLC and melting point constancy. The various synthetic reactions for the preparation of UO_2 (II)-complexes **I** and **II** are summarized in Scheme 4.
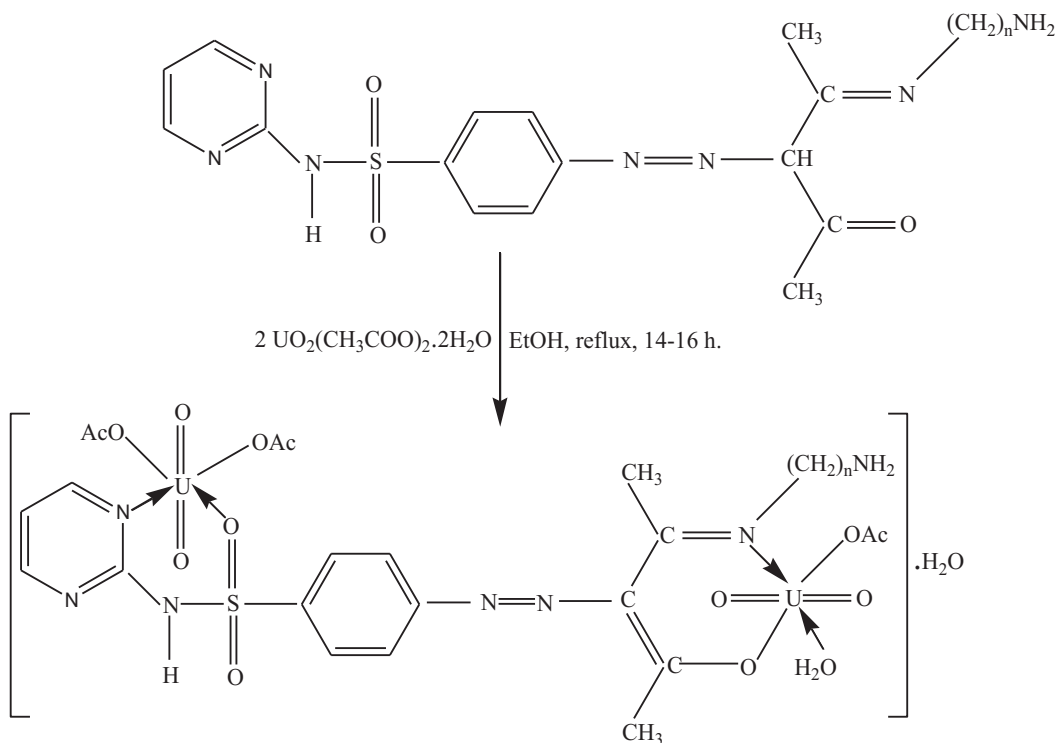
Scheme 4. Procedures for synthesis of UO_2 (II)-complexes **I** and **II** (n = 2 complex **I** and n = 6 for complex **II**).

3.4. In vitro antibacterial and antifungal assay by the Kirby–Bauer method

Antimicrobial activities of the investigated sulfadiazine azo-azomethines dyes and UO_2 (II)-complexes were determined using a modified Kirby–Bauer disc diffusion method,[54] at the micro-analytical unit of Cairo University. First 100 μL of the test bacteria/fungi were grown in 10 mL of fresh media until they reached 106 cells mL^{-1} for bacteria and 105 cells mL^{-1} for fungi.[49] Then 100 μL of microbial suspension was spread onto agar plates corresponding to the broth in which they were maintained. Isolated colonies of each organism that might play a pathogenic role were selected from primary agar plates and tested for susceptibility by the disc diffusion method.[55] From the many media available, the NCCLS recommends Mueller–Hinton agar since it results in good batch-to-batch reproducibility. The disc diffusion method for filamentous fungi used the approved standard method (M38-A) developed by the NCCLS[56] for evaluating the susceptibilities of filamentous fungi to antifungal agents. The disc diffusion method for yeasts used the approved standard method (M44-P) developed by the NCCLS.[57] Plates inoculated with the filamentous fungus *A. flavus* NRRL 6554 were incubated at 25 °C for 48 h, plates inoculated with gram-positive bacteria as *S. aureus* NCTC 6356 and gram-negative bacteria as *E. coli* NRRL-B-3704 were incubated at 35–37 °C for 24–48 h, and plates inoculated with the yeast *C.*

albicans ATCC 10231 was incubated at 30 °C for 24–48 h, and then the diameters of the inhibition zones were measured in millimeters.[58] Standard discs of tetracycline (an antibacterial agent) and amphotericin B (antifungal agent) served as positive controls for antimicrobial activity, while filter discs impregnated with 10 μL of solvent (distilled water or DMSO) were used as negative controls. The agar used was Mueller–Hinton agar rigorously tested for composition and pH. The depth of the agar in the plate is a factor to be considered in the disc diffusion method. This method is well-documented and standard zones of inhibition have been determined for susceptible and resistant values. Blank paper discs (Schleicher & Schuell, Spain) with a diameter of 8.0 mm were impregnated with 10 μL of testing concentration of the stock solutions. When a filter paper disc impregnated with a tested chemical is placed on agar the chemical diffuses from the disc into the agar, placing the chemical in the agar only around the disc. The solubility of the chemical and its molecular size will determine the size of the area of chemical infiltration around the disc. If an organism is placed on the agar, it will not grow in the area around the disc if it is susceptible to the chemical. This area of no-growth around the disc is known as a 'zone of inhibition' or 'clear zone'. For disc diffusion, the zone diameters were measured with slipping calipers of the National Committee for Clinical Laboratory Standards.[58] Agar-based methods such as E-test and disc diffusion can be good alternatives because they are simpler and faster than broth-based methods.[59]

4. Conclusion

Sulfadiazine azo-azomethine dyes (HL^I and HL^{II}) and their UO_2(II)-complexes were synthesized and characterized. Satisfactory analytical data, molar conductance measurements, magnetic susceptibility, and TOF-mass, IR, UV-Vis, and ^{1}H NMR spectral studies confirm octahedral geometry in UO_2(II)-complexes. HL^I and HL^{II} coordinate to the metal ions via a nitrogen atom of the pyrimidine ring, the oxygen atom of sulfonamide group, azomethine-N, enolic-OH formed through a keto–enol tautomerism of C=O groups in two chelation centers forming bi-homonuclear UO_2(II)-complexes. Molar conductivity values revealed that the complexes are non-electrolytes. The thermal data confirmed the suggested formula, based on spectral results. The investigated compounds were active against bacteria (*E. coli* and *S. aureus*) and fungi (*A. flavus*). The obtained data prove the usefulness of UO_2(II)-complexes as broad spectrum antimicrobial agents. Such metal complexes find wide interest, especially due to their potential as biocides and nematicides with unique electrical and magnetic properties.[60]

Acknowledgment

References

1. WHO Model List of Essential Medicines". *World Health Organization*. October 2013. Retrieved 22 April 2014.

2. Peters, A. T.; Freeman H. S. *Colour Chemistry, the Design and Synthesis of Organic Dyes and Pigments*. London, UK: Elsevier, 1991.

3. Kocaokutgen, H.; Gur, M.; Soylu M. S.; Lonnecke, P. *Dyes Pigments* **2005**, *67*, 99–103.

4. Gregory, P. *High-Technology Applications of Organic Colorants*. New York, NY, USA: Plenum Press, 1991.

5. Catino, S. C.; Farris, R. E. in: *Concise Encyclopedia of Chemical Technology*. New York, NY, USA: Wiley, 1985.

6. Ollgaard, H.; Frost, L.; Galster, J.; Hansen, O. C. *Survey of Azo-Colorants in Denmark: Consumption, Use, Health and Environmental Aspects.* Ministry of Environment and Energy, Denmark and the Danish Environmental Protection Agency, No. XX, 1998.

7. Dhar, D. N.; Taploo, C. L. *J. Sci. Ind. Res.* **1982**, *4*, 501–506.

8. Przybylski, P.; Huczyński, A.; Pyta, K.; Brzezinski, B.; Bartl, F. *Curr. Org. Chem.* **2009**, *4*, 124–148.

9. El-Medani S. M.; Ali, O. A. M.; Ramadan, R.M. *J. Mol. Struct.* **2005**, *738*, 171–177.

10. Tofazzal, M.; Tarafder, H.; Ali, M. A.; Saravana, N.; Weng, W. Y.; Kumar, S.; Tsafe, N. U.; Crouse, K. A. *Transit. Met. Chem.* **2000**, *25*, 295–298.

11. Colman, J.; Hegedu L. S. *Principles and Applications of Organotransition Metal Chemistry.* Herndon, VA, USA: University Science Book, 1980.

12. Malina, J.; Farrell, N. P.; Brabec, V. *Inorg. Chem.* **2014**, *53*, 1662–1670.

13. Nkoana, W.; Nyoni, D.; Chellan, P.; Stringer, T.; Taylor, D.; Smith, P. J.; Hutton, A. T.; Smith, G. S. *J. Organomet. Chem.* **2014**, *752*, 67–75.

14. Chellan, P.; Land, K. M.; Shokar, A.; A. Au, S.H. An, D. Taylor, D.; Smith, P. J.; Riedel, T.; Dyson, P. J.; Chibale, K.; Smith, G. S. *Dalton Trans.* **2014**, *43*, 513–526.

15. Khedr, A. M.; Marwani, H. M. *Int. J. Electrochem. Sci.* **2012**, *7*, 10074–10093.

16. Sato, H.: Morimoto, K.; Mori, Y.; Shinagawa, Y.; Kitazawa, T.; Yamagishi, A. *Dalton Trans.* **2013**, *42*, 7579–7585.

17. Klingele, J.; Dechert, S.; Meyer, F. *Coord. Chem. Rev.* **2009**, *253*, 2698–2741.

18. Saha, M.; Nasani, R.; Das, M.; Mahata, A.; Pathak, B.; Mobin, S. M.; Carrella, L. M.; Rentschler, E.; Mukhopadhyay, S. *Dalton Trans.* **2014**, *43*, 8083–8093.

19. Khedr, A. M.; Draz, D. F. *J. Coord. Chem.* **2010**, *63*, 1418–1429.

20. Issa, R. M.; Azim, S. A.; Khedr, A. M.; Draz. D. F. *J. Coord. Chem.* **2009**, *62*, 1859–1870.

21. Issa, R. M., Khedr, A. M.; Tawfik, A. *Synth. React. Inorg. Met.-Org. Chem.* **2004**, *34*, 1087–1104.

22. Ismail, T. M.; Khedr, A. M.; Abu-El-Wafa, S. M.; Issa, R. M. *J. Coord. Chem.* **2004**, *57*, 1179–1190.

23. Saad, F. A. *Spectrochim. Acta A* **2014**, *128*, 386–392.

24. Al-Ashqer, S.; Abou-Melha, K. S.; Al-Hazmi G. A. A.; Saad, F. A.; El-Metwaly, N. M. *Spectrochim. Acta A* **2014**, *132*, 751–761 .

25. Knight, J. C.; Wuest, M.; Saad, F. A.; Wang, M.; Chapman, D. W.; Jans, H. S.; Lapi, S. E.; Kariuki, B. M.; Amoroso, A. J.; Wuest, F. *Dalton Trans.* **2013**, *42*, 12005–12014.

26. Saad, F. A.; Knight, J. C.; Kariuki, B. M.; Amoroso, A. J. *Dalton Trans.* **2013**, *42*, 14826–14835.

27. Saad, F. A.; Buurma, N. J.; Amoroso, A. J.; Knight, J. C.; Kariuki, B. M. *Dalton Trans.* **2012**, *41*, 4608–4617.

28. Knight, J. C.; Saad, F. A.; Amoroso, A. J.; Kariuki, B. M.; Coles, S. J. *Acta Cryst.* **2009**, *E65*, o647.

29. Maurya, R. C.; Rajput, S. *J. Mol. Struct.* **2006**, *94*, 24–34.

30. Tas, E.; Aslanoglu, M.; Kilic, A.; Kaplan, O.; Temel, H. *J. Chem. Res-(s).* **2006**, *4*, 242–245.

31. Vogel, A. I. A. *Hand Book of Quantitative Inorganic Analysis.* 2nd Edn., London, UK: Longman, 1966.

32. Mishra, A. P.; Mishra, R. K.; Shrivastava, S. P. *J. Serb. Chem. Soc.* **2009**, *74*, 523–535.

33. Badea, M.; Emandi, A.; Marinescu, D.; Cristurean, A.; Olar, R.; Braileanu, A.; Budrugeac, P.; Segal, E. *J. Therm. Anal. Calorim.* **2003**, *72*, 525–531.

34. Khedr, A. M.; Gaber, M.; Diab H. A. *J. Coord. Chem.* **2012**, *65*, 1672–1672.

35. Singh, B. K.; Mishra, P.; Garg, B. S. *Transit. Met. Chem.* **2007**, *32*, 603–614.

36. El-Baradie, K. Y.; Gaber, M. *Chem. Pap.* **2003**, *57*, 317–321.

37. Mohamed, G. G.; Gad-Elkareem, M. A. M. *Spectrochim. Acta A* **2007**, *68*, 1382–1387.

38. Agarwal, R. K.; Agarwal, H. *Synth. React. Inorg. Met.-Org. Chem.* **1996**, *26*, 1163–1177.

39. Nakamoto, K. *Infrared and Raman Spectra of Inorganic and Coordination Compounds.* New York, NY, USA: Wiley, 1986.

40. Sharaby, C. M.; Mohamed, G. G.; Omar, M. M.; *Spectrochim. Acta A* **2007**, *66*, 935–948.

41. Mostafa, S. I. *Transit. Met. Chem.* **1998**, *23*, 397–401.

42. Cukuravali, A.; Yilmaz, I.; Kirbag, S.; *Transit. Met. Chem.* **2006**, *31*, 207–213.

43. Chandra, R. *Synth. React. Inorg. Met.-Org. Chem.* **1990**, *20*, 645–659.

44. Dash, D. C.; Mahapatra, A.; Naik, P.; Mohapatra, P. K.; Naik, S. K. *J. Korean Chem. Soc.* **2011**, *55*, 412–417.

45. El-Tabl, A. S.; El-Saied, F. A.; Al-Hakimi, A. N. *Transit. Met. Chem.* **2007**, *32*, 689–701.

46. Abdallah, S. M.; Zayed, M. A.; Mohamed, G. G. *Arabian J. Chem.* **2010**, *3*, 103–113.

47. Hart, F. A.; Newbery, J. E.; Shaw, D. *Chem. Commun. (London)*, **1967**, *1*, 45–46.

48. Phaniband, M. A.; Dhumwad, S. D. *Transit. Met. Chem.* **2007**, *32*, 1117–1125.

49. Pfaller, M. A.; Burmeister, L.; Bartlett, M. S. *J. Clin. Microbiol.* **1988**, *26*, 1437–1441.

50. Thimmaiah, K. N.; Lloyd, W. D.; Chandrappa, G. T. *Inorg. Chim. Acta* **1985**, *106*, 81–83.

51. Collins, C. H.; Lyne, P. M. *Microbiological Methods*, London, UK: Butterworth, 1976.

52. Kulkarni, A.; Avaji, P. G.; Bagihalli, G. B.; Patil, S. A.; Badami, P. S. *J. Coord. Chem.* **2009**, *62*, 481–492.

53. Mijin, D.; Uscumlic, G.; Perisic-Janjic, N.; Trkulja, I.; Radetic, M.; Jovancic, P. *J. Serb. Chem. Soc.* **2006**, *71*, 435–444.

54. Bauer, A. W.; Kirby, W. M.; Sherris, C.; Turck, M. *Am. J. Clin. Path.* **1966**, *45*, 493–496.

55. National Committee for Clinical Laboratory Standards. Performance antimicrobial susceptibility of Flavobacteria, 41, 1997.

56. National Committee for Clinical Laboratory Standards. Reference method for broth dilution antifungal susceptibility testing of conidium-forming filamentous fungi: Proposed Standard M38-A. NCCLS, Wayne, PA, USA, 2002.

57. National Committee for Clinical Laboratory Standards. Method for antifungal disk diffusion susceptibility testing of yeast: Proposed Guideline M44-P. NCCLS, Wayne, PA, USA, 2003.

58. National Committee for Clinical Laboratory Standards. Methods for dilution antimicrobial susceptibility tests for bacteria that grow aerobically. Approved standard M7-A3. National Committee for Clinical Laboratory Standards, Villanova, PA, USA, 1993.

59. Liebowitz, L. D.; Ashbee, H. R.; Evans E. G.; Chong, Y.; Mallatova, N.; Zaidi, M.; Gibbs, D. *Diagn. Microbiol. Infect. Dis.* **2001**, *40*, 27–33.

60. Jain, M.; Gaur, S.; Singh, V. P.; Singh, R. V *Appl. Organomet. Chem.* **2004**, *18*, 73–82.